Gheorghe Bunget[1]
Department of Engineering Physics,
Institute of Engineering,
Murray State University,
Murray, KY 42071
e-mail: gbunget@murraystate.edu

Stanley Henley
Department of Engineering Physics,
Institute of Engineering,
Murray State University,
Murray, KY 42071
e-mail: shenley1@murraystate.edu

Chance Glass
Department of Engineering Physics,
Institute of Engineering,
Murray State University,
Murray, KY 42071
e-mail: cglass8@murraystate.edu

James Rogers
Department of Engineering Physics,
Institute of Engineering,
Murray State University,
Murray, KY 42071
e-mail: jrogers@murraystate.edu

Matthew Webster
Performance Systems and Analytics,
Luna Innovations, Inc.,
Roanoke, VA 22903
e-mail: websterm@lunainc.com

Kevin Farinholt
Performance Systems and Analytics,
Luna Innovations, Inc.,
Roanoke, VA 22903
e-mail: farinholtk@lunainc.com

Fritz Friedersdorf
Performance Systems and Analytics,
Luna Innovations, Inc.,
Roanoke, VA 22903
e-mail: friedersdorf@lunainc.com

Marc Pepi
US Army Research Laboratory,
Aberdeen Proving Ground, MD 21005
e-mail: marc.s.pepi.civ@mail.mil

Anindya Ghoshal
US Army Research Laboratory,
Aberdeen Proving Ground, MD 21005
e-mail: anindya.ghoshal.civ@mail.mil

Siddhant Datta
Department of Mechanical
and Aerospace Engineering,
Arizona State University,

Decomposition Method to Detect Fatigue Damage Precursors in Thin Components Through Nonlinear Ultrasonic With Collinear Mixing Contributions

Cyclic loading of mechanical components promotes the formation of dislocation substructures in metals as precursors to crack nucleation leading to final failure of the metallic components. It is well known within the ultrasonic community that the acoustic nonlinearity parameter is a meaningful indicator of the microstructural damage accumulation. However, current nonlinear ultrasonic techniques suffer from response saturation and limited resolution after 50% fatigue life of the metallic medium. The present study investigates the feasibility of incorporating collinear wave mixing interactions into second harmonic assessments to improve the sensitivity of the nonlinear parameter to a microstructural accumulation of damage precursors (DP). To this end, a decomposition technique was explored to obtain higher harmonics from short time-domain pulses propagating through thin metallic components such as jet engine turbine blades. The results demonstrate the effectiveness of the decomposition technique to measure the acoustic nonlinearity parameter as an early and continuous indicator of fatigue damage precursors throughout the service life of critical aircraft components. A micrographic study showed a strong correlation between the nonlinearity parameter and the increase in damage precursors throughout the life of the specimens. [DOI: 10.1115/1.4045960]

Keywords: aerospace engineering, diagnostic feature extraction, failure analysis, materials testing, nonlinear ultrasonic, ultrasonics

[1]Corresponding author.
Manuscript received August 27, 2019; final manuscript received December 25, 2019; published online January 13, 2020. Assoc. Editor: Zhongqing Su.

Tempe, AZ 85281
e-mail: sdatta10@asu.edu

Aditi Chattopadhyay
Department of Mechanical
and Aerospace Engineering,
Arizona State University,
Tempe, AZ 85281
e-mail: aditi@asu.edu

1 Introduction

Two primary damage mechanisms threaten the integrity of jet engine components: cumulative deterioration of the microstructure through creep and fatigue. The latter occurs through thermal and mechanical cyclic loading. These modes of failure depend not only on the material, but also on the operating cycles, high-frequency vibrations, temperature, and environment. The progression of the microscopic damage leads to the formation of micro- and macrocracks. Yet, for most metallic materials, it takes approximately 80% or more of the entire fatigue life for a crack to nucleate and grow to a detectable size [1]. If left undetected, these cracks will ultimately result in catastrophic failure of the engine.

To avoid engine failure, periodic component inspections are essential for assessing degradation and estimating remaining useful life. Significant cost-savings can be achieved by maximizing the interval between inspections but doing so requires sufficient sensitivity to allow damage to be identified at its mitigation stage. Cyclic thermo-mechanical loadings during the service life of engine components promote the formation of atomic dislocations of the crystal lattice and their motion through the microstructural domain prior to the formation of macroscopic damage, i.e., cracks. Cantrell and Yost [2] associated the dislocation motion with the local strain of the material. Based on early research, Cantrell [3] divided the process of cyclic stress-induced fatigue into roughly four stages of damage progression: cyclic hardening/softening, strain localization and microcrack nucleation, macrocrack formation through the coalescence of microcracks, crack propagation, and fracture. This entire process is dominated by the formation and organization of lattice dislocations. Together with adiabatic shear bands, crazing, slip bands, residual stresses, and inclusions, crystal dislocations are generally categorized as damage precursors.

While these so-called damage precursors can be detected through microscopy, positron annihilation, and acoustic reverberation, these techniques are expensive, laborious, and not suited for the automated scanning of individual engine parts. Ultrasonic techniques offer a more attractive and nondestructive way to assess microstructural degradation related to early-stage damage. Ultrasonic waves propagating in polycrystalline materials undergo scattering phenomena from crystallites (grains), precipitates, and lattice imperfections, such as dislocations, slip bands, dislocation cells, and dislocation pileup at grain boundaries. Understanding the progression of these damage precursors has been instrumental in the past and current research aimed at understanding the attenuation observed in linear ultrasonic measurements due to scattering mechanisms within the microstructure. Granato and Lücke [4] developed a string model and formulated a change in the acoustic attenuation that was sensitive to the dislocation buildup in fatigued metals. More recently, Rose [5,6] proposed a model of ultrasonic backscattering to quantify the size of equiaxed grains. His theory was further developed by Panetta et al. [7] and applied to map grain sizes in Nickel-base superalloys for turbine disks.

While ultrasonic backscatter techniques proved successful in sizing grains of 3 μm based on linear ultrasonic analysis, the nonlinear ultrasonic (NLU) techniques have further improved the resolution with sensitivity to nano-scale features within the microstructure of solids [8]. The research led by Breazeale and coauthors [9–11] and Hikata and coauthors [12–14] are regarded as among the pioneering works in NLU. They observed that when a monochromatic sinusoidal waveform was transmitted inside a material, the output was a form that contained higher harmonic terms. Hikata et al. [12] described how higher harmonics could be generated due to the dislocation damping effect on the monochromatic waveform. More recently, NLU techniques have been successfully used by several research teams and in academic circles to track microstructural changes related to thermal aging [15], fatigue [16,17], and creep [18–20] mechanisms.

Yet, NLU techniques pose challenges due to the low amplitude of the higher harmonic content and the need to accurately extract harmonic amplitudes from the frequency spectrum of received waveforms. NLU techniques based on a through transmission arrangement, in which longitudinal waves are propagated through a sample from a transmitter to a receiver, often suffer from a wide frequency spectrum associated with the first harmonic which causes it to overlap the second harmonic due to a limited number of cycles that can be transmitted through without interference. This is particularly true of thin components. The most straightforward way to narrow the frequency spectrum in order to reduce harmonic overlap is to transmit long tonebursts. Yet in practice, such long tonebursts are often only feasible in inspections having long propagation distances such as those using surface or Lamb waves. These techniques have proven effective at tracking fatigue damage as demonstrated by Kim et al. [17] for Ni-base superalloys when using Rayleigh surface waves, or Lamb-guided waves as indicated by Pruell et al. [21], Lissenden et al. [22], and Pruell et al. [23] in aluminum plates. Yet, Rayleigh waves only interrogate the surface of a component to the depth of one wavelength, which is usually less than a few millimeters, and Lamb waves are limited in their applications since very few sets of wave modes fulfill the requirements for cumulative propagation. Furthermore, Rayleigh and Lamb waves need a minimum propagation distance and are not be suitable for thin and short components as in the case of hot section turbine blades. Most importantly, the resulting measured material nonlinearity with these techniques is an average over the propagation distance and cannot be localized.

In parallel with the recent development in the field of harmonic generation, the feasibility of using nonlinear collinear wave mixing techniques has been investigated by several researchers as a way to localize nonlinearity assessments and to overcome many of the limitations associated with harmonic generation. Li et al. [24] and Xavier et al. [25] demonstrated its potential to measure the absolute nonlinearity of relatively thick aluminum and titanium specimens, while Liu et al. [26] tracked plastic deformation in aluminum. For practical reasons, the authors of this study investigated the feasibility of using a simplified collinear mixing technique where only a single longitudinal wave transmitter is used in a pulse-through configuration. Yet, the instrument damping is adjusted so that the direct path pulse has a transient ringing portion long enough to mix with the first backwall reflection. This simplified collinear mixing induces a weaker than usual mixing condition but is added to the conventional harmonic generation response to improve the sensitivity to the development of pre-cracking fatigue damage.

A goal of this study is to enable the analysis of damage precursors accumulation locally in thin specimens; thus, the development of

signal processing techniques capable of separating the harmonics associated with the short tonebursts needed for pulse-through longitudinal wave inspections is of paramount importance. Recent research investigations by the authors and collaborators sought to find alternatives to the classical Fourier Transform analysis. Yee et al. [27] and Bunget et al. [28,29] proposed a comparison of the measured ultrasonic waves with synthetic sinusoidal wave packets in which the similarity of the waveforms is assessed based on cross-correlation techniques. These techniques were successfully applied to track fatigue damage in thin (3-mm thick) Ni-base superalloys. More recently, Scott et al. [30] investigated other signal processing alternatives such as least-squares and Prony method. However, although their proposed techniques applied excitation signals like those that would be required for thin specimens, they have only been demonstrated on relatively thick specimens.

In this paper, a nonlinear technique with collinear mixing contributions is applied to assess the fatigue level in Ni-base superalloys. A nonlinear parameter is introduced using cross-correlation with sinusoidal packets. The proposed parameter is experimentally measured and used to assess fatigue level in a library of mechanically fatigued Inconel 718 specimens. A micrographic study of fatigue damage progression is presented as a validation of ultrasonic sensitivity to damage precursors.

2 Theoretical Background

To illustrate the detection mechanisms of NLU, consider a finite amplitude plane-wave of frequency f that travels through a metallic material. Experimentally, it has been observed that part of the acoustic energy of frequency f (the fundamental component) transfers to its higher harmonic states ($2f$, $3f$, …) that are generated during wave propagation. This is a classic effect of nonlinearity that appears in many dynamic systems. In NLU assessments, this enables researchers to detect the early signs of damage as the energy transfer to higher harmonics occurs proportionally to the amount of material nonlinearity related by the accumulation of damage precursors. The known Hooke's stress–strain relation of the oscillating material particles can be written in the nonlinear form as a power series expansion [12]

$$\sigma = A\varepsilon + \frac{1}{2}B\varepsilon^2 + \cdots \tag{1}$$

where σ is the stress created by the propagating wave oscillating the metallic particles with a displacement gradient, i.e., strain, $\varepsilon = \partial u/\partial x$, and A and B are coefficients of the second- and third-order terms of the power series. Assuming 1D wave propagation in the x-direction, the oscillating motion of the metallic particles is described by the wave equation

$$\rho\frac{\partial^2 u}{\partial t^2} = \frac{\partial \sigma}{\partial x} \tag{2}$$

where ρ is the material density and $u = A_1 \sin \omega t$ is the particle displacement when the wave with the amplitude A_1 and the angular frequency ω propagate through the metallic medium. Plugging stress from (1) into (2) and applying 1D strain–displacement relations, one gets

$$\rho\frac{\partial^2 u}{\partial^2 t} = A\frac{\partial^2 u}{\partial x^2} + B\frac{\partial u}{\partial x}\frac{\partial^2 u}{\partial x^2} \tag{3}$$

This nonlinear differential Eq. (3) can be solved approximately by iterations [12]. After two iterations, one gets

$$u(x, t) = A_1 \sin(kx - \omega t) - \frac{1}{8}\frac{B}{A}k^2A_1^2 x\cos[2(kx - \omega t)] + \cdots \tag{4}$$

where $k = 2\pi/\lambda$ is the wave number, λ is the wavelength of the fundamental amplitude, and x is the propagation distance of the waveform. The second term has the frequency 2ω and represents the second harmonic of the waveform that is generated by the nonlinearities (inhomogeneities) present in the metallic medium. The amplitude of this second term can be written as [31]

$$A_2 = \frac{1}{8}\left(\frac{B}{A}\right)A_1^2\, k^2 x \tag{5}$$

The term B/A in Eq. (5) represents the known nonlinearity parameter, β, and rearranging the terms in Eq. (5), we arrive at a common form as

$$\beta = \frac{A_2}{A_1^2}\left(\frac{8}{k^2 x}\right) \tag{6}$$

When applied to longitudinal waves in isotropic materials, Breazeale and coauthors [32,33] related the nonlinearity parameter to other second- and third-order material elastic constants such as, Lamé (λ, μ) and Murnaghan (l, m) constants

$$\beta = \frac{3}{2} + \frac{l + 2m}{\lambda + 2\mu} \tag{7}$$

The nonlinearity parameter can be calculated based on Eq. (6) from experimental measurements of absolute transducer displacements and extraction of harmonic amplitudes, A_1 and A_2. However, since the sound velocity of compressional waves is independent of the excitation frequency, and given a constant propagation distance is constant, one may use only the electrical amplitudes to perform a relative measurement of the nonlinearity parameter

$$\beta \propto \beta' = \frac{A_2'}{(A_1')^2} \tag{8}$$

For short excitation waveforms like those required for thin specimens, accurate extraction of the second harmonic amplitude, A_2', is challenging. The cross-correlation function provides a measure of how two signals are similar to each other at different points in time, which can be used to extract the harmonic amplitudes even in the case of overlapping peaks for A_1' and A_2' in the frequency domain. In NLU assessments, the measured signal, $x(t)$ recorded from the receiver can be segmented into fixed time intervals, $x_j(t)$ corresponding to received pulses of the propagating waveform. The first and second harmonic components, f_1 and $2f_1$, contained in the selected analysis region can be recovered through the cross-correlation of the selected signal with synthetic sinusoids of frequencies, f_1 and $2f_1$.

Given the received waveform, $x(t)$, a segment of its signal, $x_j(t)$, is selected for the nonlinear analysis starting at a receiving delay, t_r. Assume that the segment has a time-length T, its evaluation is performed between the times t_r and $t_r + T$. Consider two real, stationary, zero-mean sinusoidal wavelets $y_j(t) = \sin(2\pi \cdot f_{Aj} \cdot t)$ as two monochromatic sinusoids representing the simulated first and second harmonics of the received signal. The relative amplitudes A_1' and A_2' are evaluated from the frequency spectra of the convolution functions of the segmented signal $x_j(t)|_{t_r}^{t_r+T}$ with the monochromatic packets:

$$\begin{aligned} r_1(t) &= \frac{1}{\Delta t}\int_{t_r}^{t_r+T} x_j(t)\cdot y_{f_1}(t+\tau)\cdot dt \\ r_2(t) &= \frac{1}{\Delta t}\int_{t_r}^{t_r+T} x_j(t)\cdot y_{f_2}(t+\tau)\cdot dt \end{aligned} \tag{9}$$

where the amplitudes A_1' and A_2' are calculated as the amplitudes of the steady-state portions of $r_1(t)$ and $r_2(t)$, respectively.

3 Materials and Methods

The harmonic generation technique combined with a simplified collinear wave mixing was used to measure the acoustic nonlinearity parameter [12]. The core component of the nonlinear ultrasonic system was a SNAP 5000 RAM (Ritec Inc., Warwick, RI) capable

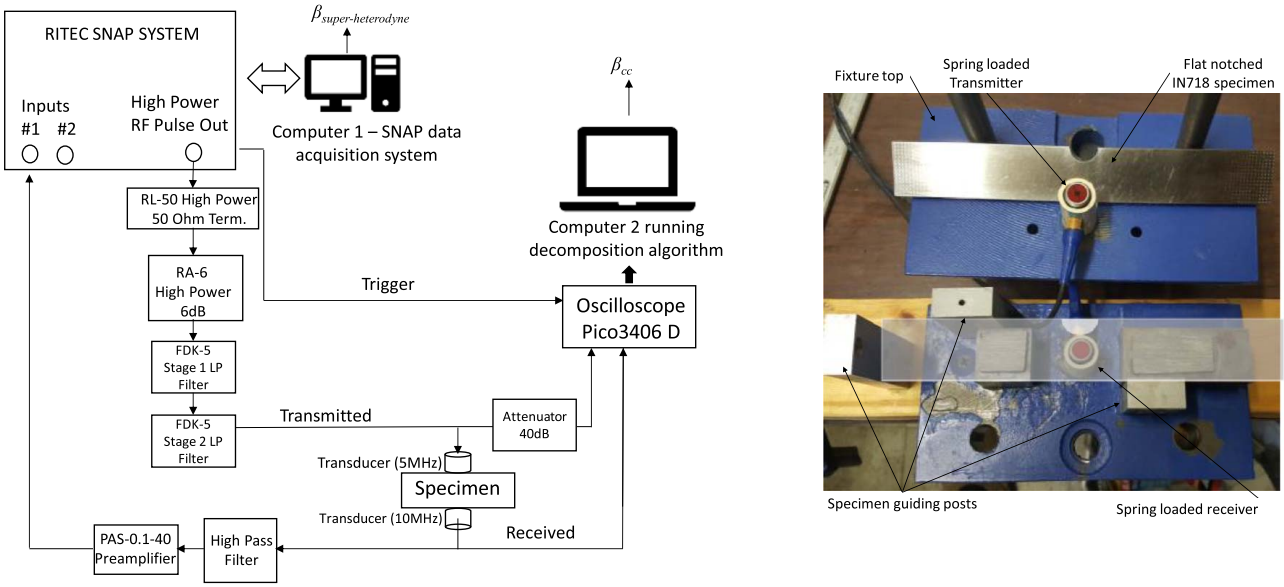

Fig. 1 Experimental setup. Left: the Ritec setup for nonlinear measurements was adapted to record data from both the heterodyne, i.e., $\beta_{heterodyne}$, and separate data to be processed with the CC algorithm, i.e., β_{CC}. Right: IN718 specimen and transducers-specimen fixture for pulse-through measurements.

of high power (5 kW) tone burst excitations (Fig. 1, left). This nonlinear measurement system can provide monochromatic ultrasonic sine wave signals of high quality, thus decreasing considerably the acoustic nonlinearity artifacts stemming from the excitation signal. A matching network of integrated low-pass filters was used to further suppress high-frequency distortion from the instrument, and it was used to deliver a three-cycle toneburst excitation with a frequency of 5 MHz and approximately 450 Vp-p. Two broadband piezoelectric transducers were used as transmitter as receiver (Olympus NDT Panametrics, V201-RM and V202-RM, respectively). The transmitter converts the electrical signal into longitudinal ultrasonic vibration which then is transmitted into the specimen with mineral oil as the couplant. The vibration propagates inside the specimen, and it is received and transformed in electric signal at the 10 MHz receiving transmitter. The internal trigger signal from the SNAP system was used as a reference trigger to synchronize external data acquisition using a Picoscope 3406D USB oscilloscope with internal data acquisition through the SNAP system's superheterodyne receiver. A number of 100 temporal averages were used at each measurement to suppress the electrical noise. Data were recorded by using two acquisition systems: (1) the acquisition system accompanying the superheterodyne of the SNAP 5000 RAM and (2) a second system to digitize and record raw transmitted and received waveforms. The first system was used as a benchmark to compare the results measured with the second system and analyzed through the proposed cross-correlation (CC)-decomposition method.

The superheterodyne computed the total energy between 3.1 and 5 μs after the transmission ended. The energy was calculated using analog integration of the in- and out-of-phase components at the 10 MHz frequency. A specimen fixture was designed to maintain alignment parallelism between the transmitting and receiving transducers during multiple replicate measurements on the library of fatigued specimens (Fig. 1, right). The transducers were spring-loaded to maintain a repeatable contact loading between transducers and the specimens. The authors observed that during measurements a spring-loaded solution for the transducers was instrumental to increase the measurement repeatability.

A library of five flat (25.4-mm width, 150-mm long, and 3-mm thick) Ni-base superalloy IN718 with a single round notch was prepared. The specimens were not hardened, but they were solution aged and annealed prior to fatigue testing. The procedure was based on the specifications in the AMS 5596 standard and involved a heat treatment of 955 °C for 1 h in an endothermic atmosphere and a quench by rapid air cool. This was followed by an age cycle consisting of heating to 718 °C and hold for 8 h, furnace cool/ramp 2 h to the next temperature of 621 °C and hold for 8 h, then cool in ambient air. The specimens were then polished before fatigue testing to remove the oxide layer, but nothing was done to them after fatigue testing. These specimens were cyclically loaded to 20, 40, 60, and 80% fatigue life. These specimens were high-cycle fatigued in tension–tension loading with maximum stress at 37.5% (414 MPa) of the yield and a stress ratio of 0.1, leading to an estimated 75,000 cycle fatigue life with cracks nucleation occurring only after approximately 90% of the fatigue life was expended. Selected specimens were cyclically loaded to 20, 40, 60, and 80% of their fatigue life for the evaluation of damage precursor development. The experimental plan was to measure the nonlinearity parameter across the thickness of the specimens at the root of the round notch (image specimen with round transducer). The hypothesis was that the fatigue damage precursors will accumulate at the stress concentrator where the specimens had the smallest cross-sectional area. The measurements were randomly repeated four times for each specimen. Before each measurement, the transducers were wiped clean and a fresh couplant was applied.

4 Results and Discussion

In the proposed simplified collinear mixing procedure, the ringing transient portion of the transmitted waveform interacts with the reflection from the receiver interface of the direct pulse (Fig. 2, left). While the oscilloscope recordings shown in Fig. 2 (left), the two signals were recorded at separate sides of the specimen (one being delivered by the transmitter and the other as the output of the receiver), their overlap in the time domain suggests that the ringing transient portion of the transmitted waveform traveled through the thickness of the specimen at the same time as the reflection from the direct path pulse. To better illustrate the effect of wave mixing in the thin specimens that are the focus of this work, a similar measurement was performed with a specimen having twice the thickness of the specimens of the fatigued library (Fig. 2, right). In this case, the ringing transient portion of the transmitted waveform ended before the reflection from the receiver interface could reach it, and thus, no mixing occurred, and as a result, the second received pulse was identical in the form to the first received pulse.

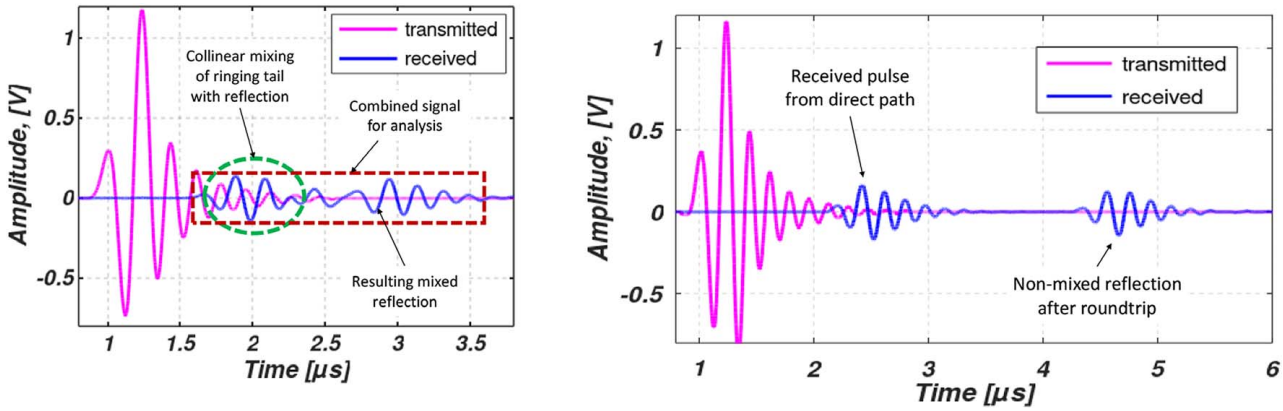

Fig. 2 Simplified collinear mixing procedure (left) as compared to a non-mixing case when transmitted wave propagates through a thicker (6.35-mm) specimen of IN718 on the right

The case of a longitudinal sinusoidal wave interacting with itself to produce a second harmonic frequency was investigated early on by Rollins [34] and based on the energy and momentum conservation a scattered wave is obtained that might be described as

$$L(\omega_1) + L(\omega_1) = L(2\omega_1) \tag{10}$$

where for our case the frequency of the direct path and the reflected echo were $\omega_1 = 2\pi \cdot 5$ MHz. The resulting recorded waveform exhibited a repeating pattern consisting of the pulses of the direct path and the collinear mixing signal (Fig. 3). Starting with the second repeating pattern in the sequence, the direct path had a 180 deg phase change since it contained reflections of the direct path and not the direct path pulse. The combined signal of the direct path and mixed reflection, i.e., the first repeating pattern, was used in the measurements based on cross-correlation decomposition.

Using the proposed decomposition technique, typical cross-correlated signals, $r_1(t)$ and $r_2(t)$ were obtained for long synthetic sinusoids, 40 and 80 cycles (Fig. 4). The whole time-domain lengths of these signals consist of cross-correlation transient portions and a stable steady-state portion in the middle. The steady-state portion is so stable that there is no need to perform a Fourier transform in order to obtain the amplitudes, $(A_1)_{CC}$ and $(A_2)_{CC}$, of these sinusoidal waves. These uncalibrated relative amplitudes are proportional to the particle displacements $u(x,t)$ represented in Eqs. (2)–(4) and can be used to calculate a relative nonlinearity parameter, β_{CC}

$$\beta_{CC} = \frac{(A_2)_{CC}}{(A_1^2)_{CC}} \tag{11}$$

For practical reasons, calibration blocks that are representative of non-fatigued material could be used in a calibration procedure of different excitation values, transducers, and lengths of synthetic sinusoids.

A baseline analysis of the sample population was made by using the Ritec system's superheterodyne receiver to calculate the amplitude of the second harmonic component of the received signal. For this analysis, the gate of the heterodyne of the Ritec system was adjusted so that it contained the combined signal of both the direct path pulse and the reflection containing the collinear contribution. The maximum observed data spread for the heterodyne system was 17% over the full scale of the measurements and occurred only for the 80% fatigue level where the data spread was significantly larger than that for the previous levels (Fig. 2). The nonlinearity parameter, $\beta_{heterodyne}$, increased sharply along a sigmoidal trend for the early stages of fatigue levels, and it became relatively insensitive to fatigue for levels larger than 60% life. The specimens

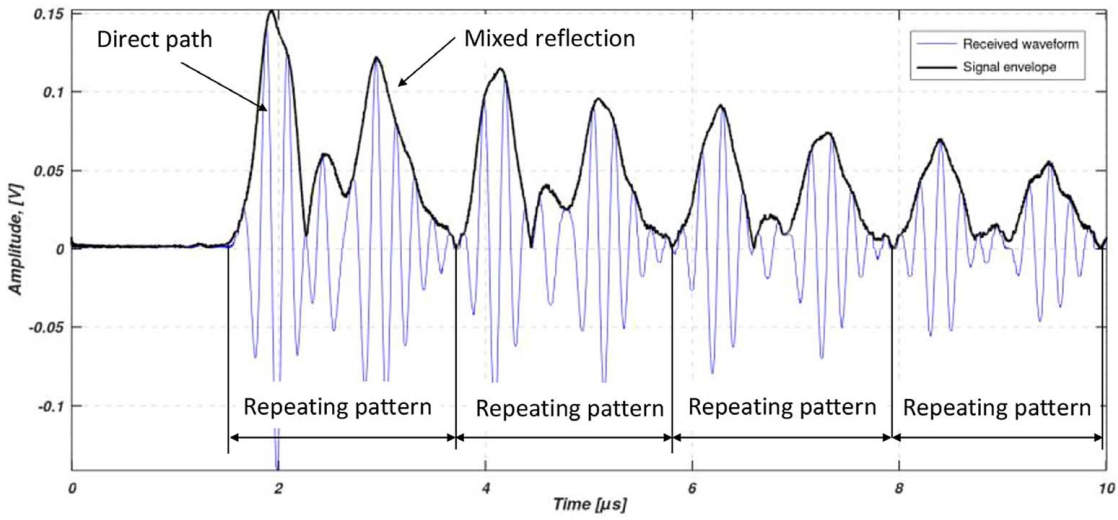

Fig. 3 The collinear mixing resulted in a repeating pattern of the direct and mixed signals that propagated multiple times through the thickness of the thin specimens. The blue curve represents multiple echoes of the received waveform and the black, thicker curve represents the envelope (analytic signal) as obtained through Hilbert transform. (Color version online.)

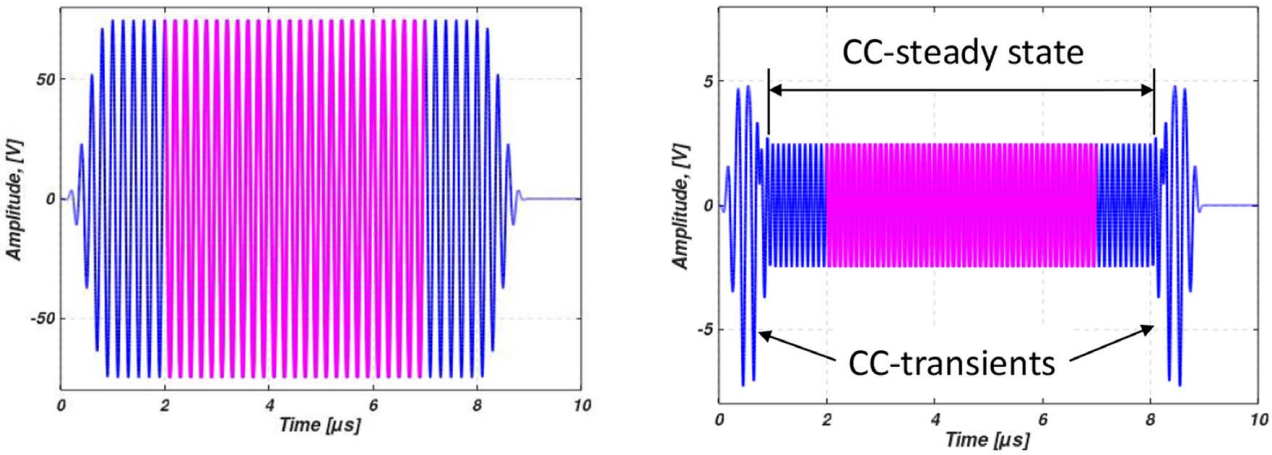

Fig. 4 Typical cross-correlated selected regions of component f_1 on the left and $2f_1$ on the right. Only the steady-state mid regions of the CC functions were used to measure the harmonic amplitudes, $(A_{CC})_1$ and $(A_{CC})_2$.

fatigued at the 80% level exhibited an increase of 300% of nonlinearity parameter over pristine specimens. This increase is mostly related to the increase of the second harmonic since, in the SNAP system, the first harmonic is measured from the excitation signal delivered to the ultrasonic transmitter, i.e., the FDK-6 stage 2 low-pass filter output and thus is not impacted by the specific specimen under test (Fig. 1). Only the second harmonic was obtained from the received waveform after its propagation through the metallic media.

The linearity of the ultrasonic measurement system and the cross-correlation procedure for the direct path and the collinear mixing of the first reflection was tested in order to verify measurement consistency and minimal influence from spurious nonlinearities. Specifically, the intent was to ensure that the measured nonlinearities were associated with the changes in the material state and not merely to the nonlinearities that are always present in the amplifier, electronics, and transducers. A simple experiment was performed by gradually increasing the amplitude of the excitation of the Ritec system. The proposed cross-correlation technique exhibited linearity comparable with that of the heterodyne Ritec system. Both techniques had a coefficient of determination for linearity larger than 0.95 (Fig. 5). Yet, the cross-correlation of the direct path received pulse and the collinear mixed reflection with sinusoidal packets had better linearity for higher excitation amplitudes.

The data variance of the measured nonlinearity based on the combined repeating pattern increased for the collinear mixing, and the full-scale measurement increased significantly when compared to the harmonic generation of the direct path. Therefore, when reported to the full scale, the maximum observed measurement variation was 28% for collinear mixing compared to 65% when using only the direct pulse. Moreover, after a sharp increase up to 30% fatigue level, the nonlinearity measurements for the direct path had the tendency to saturate over 50% of fatigue life. However, the results indicated that for the combined pulse, little or no saturation occurred over the range of fatigue levels examined. The saturation effect observed after approximately 50% fatigue in both the baseline heterodyne measurements (Fig. 6) and the direct path cross-correlation analysis (Fig. 7, left) was in agreement with that of prior research. Cantrell [35,36], Wu et al. [37] and Matikas [38] obtained a similar 50% saturation phenomenon in the case of fatigue of aluminum 2024, 410Cb stainless steel, IN100, magnesium alloys, and Ti-6Al-4V. Thus, the added contribution of collinear mixing provides an advantage over conventional harmonic generation approaches in that it could enable an effective assessment of fatigue life over the 50% level.

The CC algorithm using the collinear contribution significantly increased the sensitivity to the accumulation of damage precursors when compared to the conventional harmonic generation analyses. The sensitivity is increased in part due to the ability of the cross-correlation to decompose the original waveform to obtain harmonic amplitudes. In contrast, only the second harmonic contributes to the increase of the nonlinearity parameter in the heterodyne-based approach [2,12,39]. The CC algorithm is sensitive to the energy

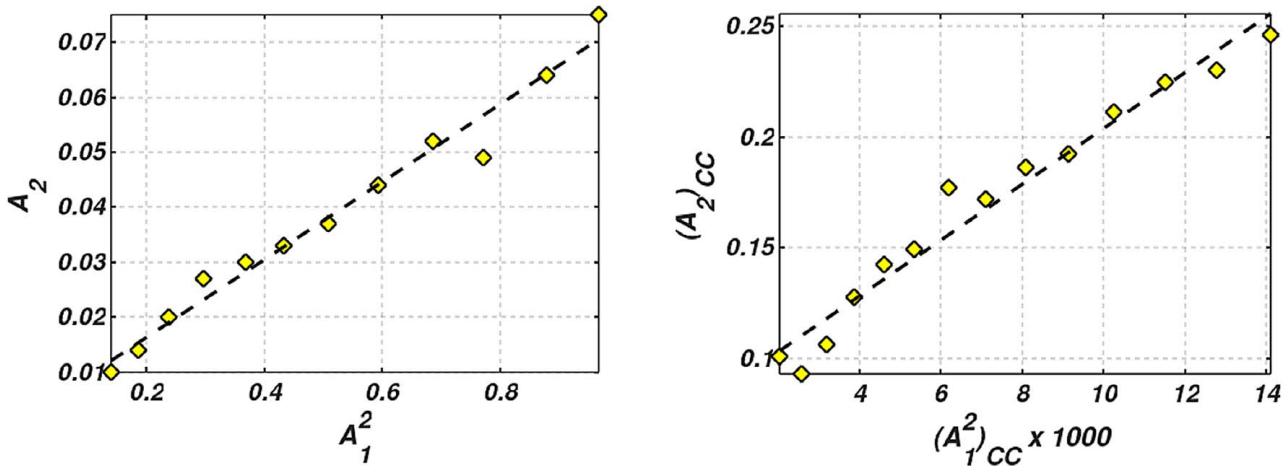

Fig. 5 Linearity and repeatability of the measurement system and proposed procedure: Ritec heterodyne procedure (left) and cross-correlation of the combined direct path and collinear mixed reflection with sinusoidal packets

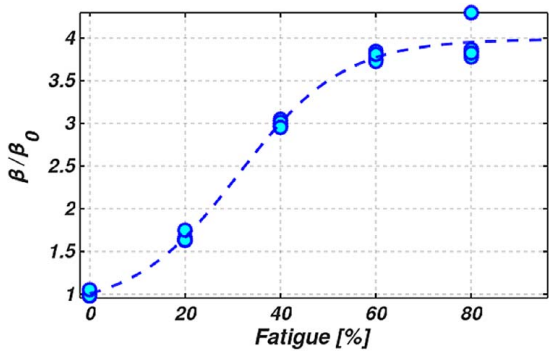

Fig. 6 Nonlinearity parameter, $\beta_{heterodyne}$, measured with the Ritec heterodyne system. Both the direct and the collinear wave mixing reflection was used for these measurements.

transfer from the first harmonic to the second harmonic. Thus, while the second harmonic increases with the level of damage, the first harmonic that is calculated through the CC procedure decreases as energy is transferred toward the second harmonic component (Fig. 8). This advantage is novel, and it is not found in more conventional analysis procedures. Figure 8 shows that the amplitude of the first harmonic decreases more than 50% at a fatigue level of 80% which may correspond to the point at which a crack could nucleate and become visible at the surface. However, we should mention that our specimens did not have any visible crack at this level of fatigue. At the same time, the second harmonic increased approximately 1300%.

The phase of the cross-correlated signals from the direct received pulse and of the first reflection containing the wave mixing contribution was measured to observe its contribution to the measured harmonic amplitudes (Fig. 9). Two methods were utilized: an overlap algorithm in the time domain and a Fourier Transform in the frequency domain. The results of both methods were in agreement. The phase shift between the reflected mixed echo and the direct path was found to be 180 deg, which was in agreement with the results obtained by Van Buren and Breazeale [40]. Yet, the phase shift between the direct path and the reflected mixed echo exhibited a strong decrease with the fatigue level, especially for the first harmonic amplitude, $(A_1)_{cc}$. The ability to perform phase measurements of higher harmonic components from experimentally measured signals, as well as the higher harmonic amplitudes of short time-domain signals, is an advantage that the presented decomposition technique provides to the signal processing of nonlinear ultrasonics.

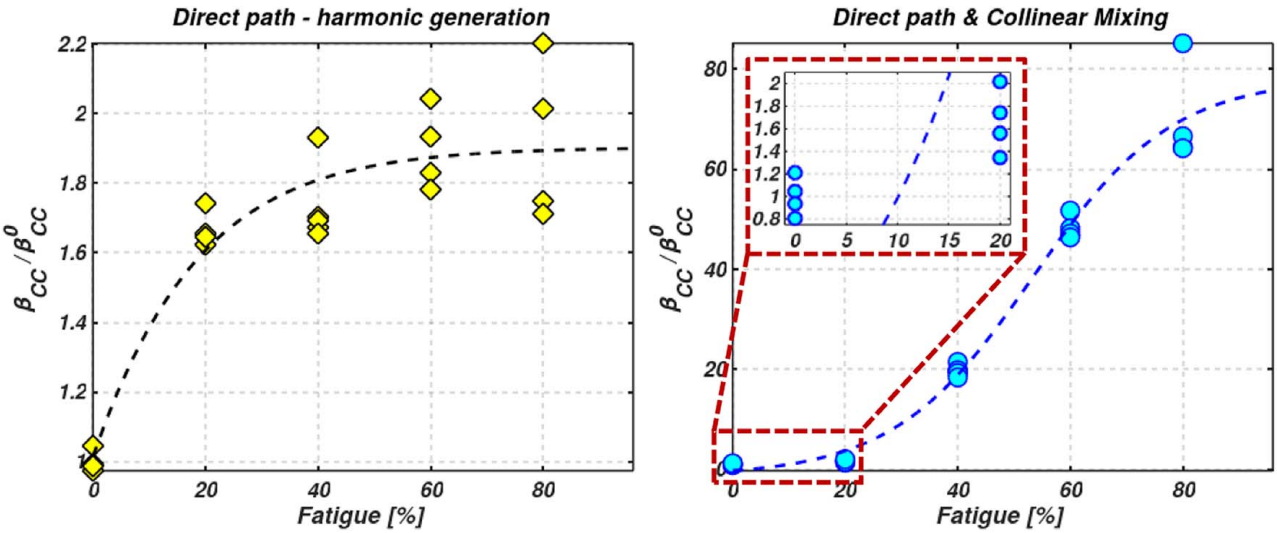

Fig. 7 The change of the relative nonlinearity parameter was significant for the first repeating pattern, i.e., the direct path and collinear mixing echo (right) when compared only to the harmonic generation of the direct path pulse (left). Both measurements were performed with harmonic amplitudes calculated through cross-correlation with sinusoidal packets.

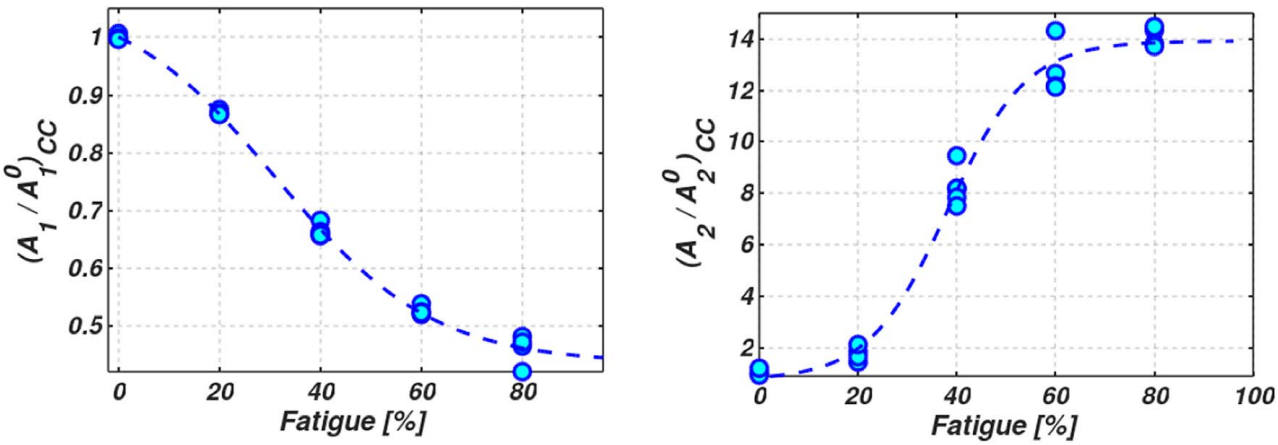

Fig. 8 The first harmonic decreased monotonically with fatigue percent life (left), while the second harmonic increased significantly (right)

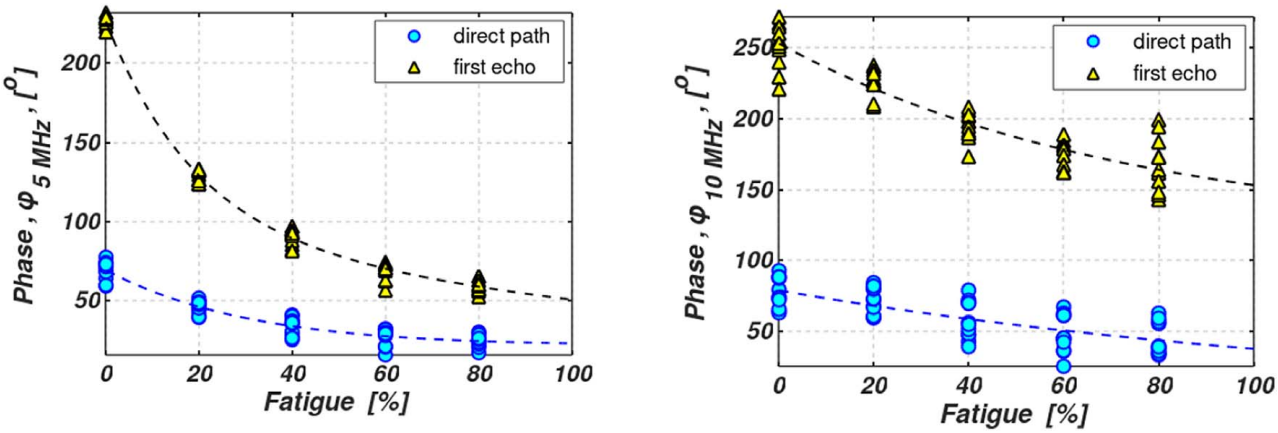

Fig. 9 The phase of the cross-correlated signals first harmonic decreased monotonically with fatigue percent life (left), while the second harmonic increased significantly (right)

In order to verify that the observed increase in the material nonlinearity was attributed to microstructural changes, transmission electron microscope (TEM) images were collected at three representative fatigue levels. Discs of 3-mm diameter were machined from the specimens using electron discharge machining. These discs were mechanically polished to a thickness of 60 μm after which electropolishing was performed using a Struer TenuPol-3 electro-polisher and an electrolyte solution of 10% perchloric acid and 90% methanol. A voltage of 30 V and a temperature of −20 °C were used. Three images with identical magnification were selected, and the average value of dislocation density was considered. Dislocations appeared as the dark lines in the bright field of the TEM images due to the Bragg diffraction of the electrons that were directed away from straight through beam (Fig. 10).

The dislocation density was estimated from TEM images based on a technique presented by Adamczyk et al. [41]. The images were prepared for dislocation density measurements by using ImageJ software (NIH). The brightness and contrast of the micrographs were adjusted so that the γ' precipitate particles and the matrix were close to white, and the remaining black pixels indicated etch pits at the intersection points of dislocations. A size threshold was used to discard the remaining noise speckle. The estimated dislocation density and the nonlinearity parameter, β_{CC}, were plotted as a function of fatigue life (Fig. 11). The error bars of the dislocation densities were calculated based on estimations from four TEM images taken from different locations of the machined discs. The chart shows a strong correlation between estimated dislocation density and the measured nonlinearity parameter, β. The dislocation density appeared to increase linearly. A similar linear trend of dislocation density was obtained by Matikas [38] for in situ measurements of Ti-6Al-4V specimens.

5 Concluding Remarks

The objective of this research investigation was to examine the feasibility of using a modified nonlinear ultrasonic approach that considers the effects of collinear wave mixing contributions and leverages cross-correlation decomposition for analyzing the fatigue state of thin Ni-base superalloy components. The higher harmonics could be discriminated from the wideband signals of short time-domain pulses by using the CC-decomposition technique. The major outcome of the decomposition technique is a significant increase in the nonlinearity parameter β_{CC} obtained from the cross-correlation of the selected signal with sinusoidal packets of specific harmonic frequencies. This increase was due not only to the increase in the second harmonic, $(A_2)_{CC}$, but also to its ability to capture the energy transfer from the fundamental waveform toward higher harmonics. Moreover, the decomposition algorithm continues to maintain the linearity of the measurement system resulting in consistent data spread. The increase in the second harmonic, $(A_2)_{CC}$, and the decrease in the first harmonic, $(A_1)_{CC}$, of the collinear mixing pulse were associated with a change in phase from the pulse of the direct path. Yet, this change in phase decreased with the fatigue level, which in turn resulted in significant changes in the harmonic amplitudes.

The results obtained through CC decomposition were in agreement with the results obtained through the Ritec heterodyne system. The heterodyne Ritec system exhibited the least spread in data with a maximum expected error of 17%. The analysis of the combined repeating pattern containing the collinear mixing contribution had a maximum measurement variation of 28% while the harmonic generation based on the first received pulse had an error of 65%. The data scatter of the cross-correlation method might be due to the couplant thickness and the coupling coefficient

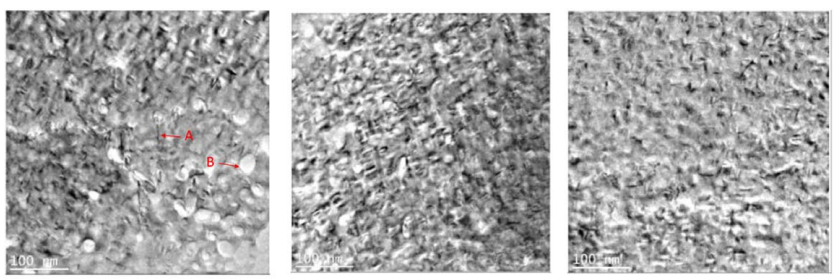

Fig. 10 TEM micrographs showing dislocations buildup, arrow A, and primary precipitates γ', arrow B, for three levels of fatigue

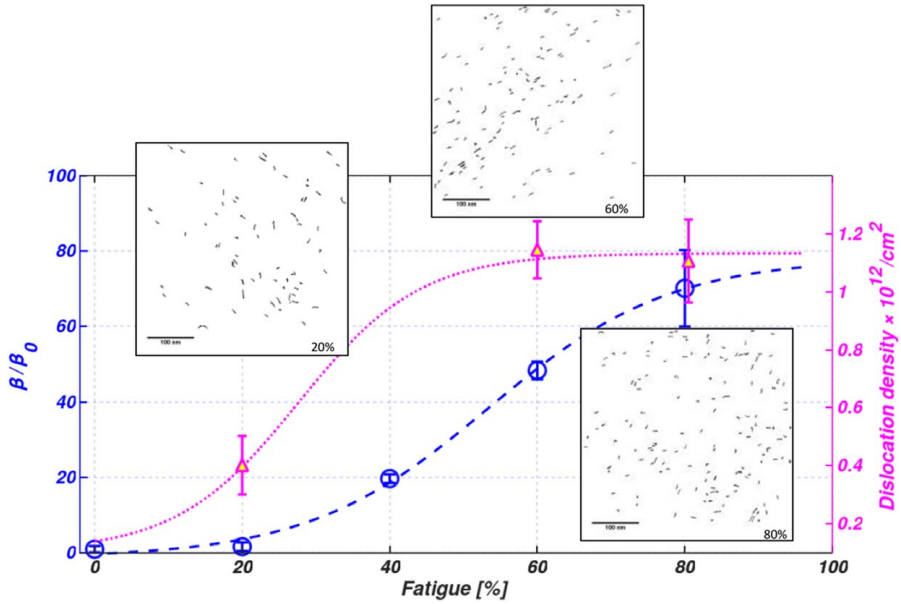

Fig. 11 Correlation between normalized nonlinearity parameter and the dislocation density as estimated from TEM micrographs that were filtered, thresholded, and watershed in IMAGEJ

between the two transducers. The couplant has a larger effect when using two pulses, i.e., the direct and the mixed reflection since the couplant interaction is located between these pulses. However, the benefit of high sensitivity to microstructural damage of the combined repeating pattern was significant (approximately 7000% increase). Moreover, its monotonic increase indicated a saturation over 80% of fatigue life as opposed to 50% for the case of harmonic generation of the first direct received pulse. This finding indicates that the nonlinearity parameter based on the CC decomposition is not only sensitive to the early stages of the fatigue process, but also during later stages of damage.

The increase in nonlinearity parameters was verified through micrographic analysis performed on TEM. A good agreement between the nonlinearity parameter, β_{CC}, and the data obtained from micrographic analysis confirm the usefulness of the decomposition technique as it was applied to the simplified collinear wave mixing. The micrographs demonstrated that the nonlinear response was greater as the damage precursor accumulated in the specimens. The authors conclude that both nonlinearity parameters, β_{CC} and $\beta_{\text{heterodyne}}$, were sensitive to the increase in the dislocation density estimated from micrographs.

Acknowledgment

The authors acknowledge the assistance of Dr. Thomas Grimsley of Ritec Inc. with the instrumentation setup and tuning.

The research reported in this document/presentation was performed in connection with contract/instrument W911QX-15-C-0024 with the U.S. Army Research Laboratory. The views and conclusions contained in this document/presentation are those of the authors and should not be interpreted as presenting the official policies or position, either expressed or implied, of the U.S. Army Research Laboratory or the U.S. Government unless so designated by other authorized documents. Citation of manufacturer's or trade names does not constitute an official endorsement or approval of the use thereof.

References

[1] Miller, K. J., 1987, "The Behaviour of Short Fatigue Cracks and Their Initiation Part II—A General Summary," Fatigue Fract. Eng. Mater. Struct., **10**(2), pp. 93–113.

[2] Cantrell, J., and Yost, W., 1994, "Acoustic Harmonic Generation From Fatigue-Induced Dislocation Dipoles," Philos. Mag. A, **69**(2), pp. 315–326.

[3] Cantrell, J. H., 2004, "Substructural Organization, Dislocation Plasticity and Harmonic Generation in Cyclically Stressed Wavy Slip Metals," Proc. R. Soc. A, **460**(2043), pp. 757–780.

[4] Granato, A., and Lücke, K., 1956, "Theory of Mechanical Damping Due to Dislocations," J. Appl. Phys., **27**(6), pp. 583–593.

[5] Rose, J., 1993, "Theory of Ultrasonic Backscatter From Multiphase Polycrystalline Solids," *Review of Progress in Quantitative Nondestructive Evaluation*, D. O. Thompson and D. E. Chimenti, eds., Vol. 12, Plenum Press, New York.

[6] Rose, J., 1992, "Ultrasonic Backscatter From Microstructure," Review of Progress in Quantitative Nondestructive Evaluation, D. O. Thompson and D. E. Chimenti, eds., Vol. 11B, Plenum Press, New York, pp. 1677–1684.

[7] Panetta, P., Bland, L., Tracy, M., and Hassan, W., 2014, "Ultrasonic Backscattering Measurements of Grain Size in Metal Alloys," TMS Annual Meeting Supplemental Proceedings, San Diego, CA, Feb. 16–20, pp. 723–730.

[8] Jhang, K., 2009, "Nonlinear Ultrasonic Techniques for Nondestructive Assessment of Micro Damage in Material: A Review," Int. J. Precis. Eng. Manuf., **10**(1), pp. 123–135.

[9] Breazeale, M. A., and Lester, W. W., 1961, "Demonstration of the "Least Stable Waveform" of Finite Amplitude Waves," J. Acoust. Soc. Am., **33**(12), p. 1803–1803.

[10] Breazeale, M., and Thompson, D., 1963, "Finite-Amplitude Ultrasonic Waves in Aluminum," Appl. Phys. Lett., **3**(5), pp. 77–78.

[11] Breazeale, M., and Ford, J., 1965, "Ultrasonic Studies of the Nonlinear Behavior of Solids," J. Appl. Phys., **36**(11), pp. 3486–3490.

[12] Hikata, A., Chick, B., and Elbaum, C., 1965, "Dislocation Contribution to the Second Harmonic Generation of Ultrasonic Wave," J. Appl. Phys., **36**(1), pp. 229–236.

[13] Suzuki, T., Hikata, A., and Elbaum, C., 1964, "Anharmonicity Due to Glide Motion of Dislocations," J. Appl. Phys., **35**(9), p. 2761–2766.

[14] Hikata, A., and Elbaum, C., 1966, "Generation of Ultrasonic Second and Third Harmonics Due to Dislocations. I," Phys. Rev., **144**(2), pp. 469–477.

[15] Barnard, D., Dace, G., and Buck, O., 1997, "Acoustic Harmonic Generation Due to Thermal Embrittlement of Inconel 718," J. Nondestr. Eval., **16**(2), pp. 67–75.

[16] Cantrell, J. H., and Yost, W. T., 2001, "Nonlinear Ultrasonic Characterization of Fatigue Microstructures," Int. J. Fatigue, **23**(Suppl. 1), pp. 487–490.

[17] Kim, J.-Y., Jacobs, L. J., Qu, J., and Littles, J. W., 2006, "Experimental Characterization of Fatigue Damage in a Nickel-Base Superalloy Using Nonlinear Ultrasonic Waves," J. Acoust. Soc. Am., **120**(3), pp. 1266–1373.

[18] Baby, S., Nagaraja Kowmudi, B., Omprakash, C. M., Satyanarayana, D. V. V., Balasubramaniam, K., and Kumar, V., 2008, "Creep Damage Assessment in Titanium Alloy Using a Nonlinear Ultrasonic Technique," Scr. Mater., **59**(8), pp. 818–821.

[19] Valluri, J., Balasubramaniam, K., and Prakash, R., 2010, "Creep Damage Characterization Using Non-Linear Ultrasonic Techniques," Acta Mater., **58**(6), pp. 2079–2090.

[20] Balasubramaniam, K., Valluri, J., and Prakash, R., 2011, "Creep Damage Characterization Using a Low Amplitude Nonlinear Ultrasonic Technique," Mater. Charact., **62**(3), pp. 275–286.

[21] Pruell, C., Kim, J.-Y., Qu, J., and Jacobs, L. J., 2009, "A Nonlinear-Guided Wave Technique for Evaluating Plasticity-Driven Material Damage in a Metal Plate," NDT&E Int., **42**(3), pp. 199–203.
[22] Lissenden, C., Liu, Y., and Rose, J., 2015, "Use of Non-Linear Ultrasonic Guided Waves for Early Damage Detection," Insight, **57**(4), pp. 206–211.
[23] Pruell, C., Kim, J.-Y., Qu, J., and Jacobs, L. J., 2009, "Evaluation of Fatigue Damage Using Nonlinear Guided Waves," Smart Mater. Struct., **18**(3), pp. 1–7.
[24] Li, P., Winfree, W., Yost, W., and Cantrell, J., 1983, "Observation of Collinear Beam-Mxing by Amplitude Modulated Ultrasonic Wave in a Solid," IEEE Ultrasonic Symposium, Atlanta, GA, Oct. 31–Nov. 2, pp. 1152–1156.
[25] Xavier, J., Barrière, C., and Royer, D., 2003, "Acoustic Nonlinearity Parameter Measurements in Solids Using the Collinear Mixing of Elastic Waves," Appl. Phys. Lett., **82**(6), pp. 886–888.
[26] Liu, M., Tang, G., Jacobs, L., and Qu, J., 2012, "Measuring Acoustic Nonlinearity Parameter Using Collinear Wave Mixing," J. Appl. Phys., **112**.
[27] Yee, A., Stewart, D., Bunget, G., Kramer, P., Farinholt, K., Friedersdorf, F., Pepi, M., and Ghoshal, A., 2017, "Nonlinear Ultrasonic Measurements Based on Cross-Correlation Filtering Techniques," AIP Conference Proceedings, Vol. 1806, Atlanta, GA, July 17–22, pp. 1–11.
[28] Bunget, G., Yee, A., Stewart, D., Rogers, J., Henley, S., Bugg, C., Cline, J., Webster, M., Farinholt, K., and Friedersdorf, F., 2018, "Flaw Characterization Through Nonlinear Ultrasonics and Wavelet Cross-Correlation Algorithms," AIP Conference Proceedings 1949, Provo, UT, July 16–21, pp. 1–10.
[29] Bunget, G., Tilmon, B., Yee, A., Stewart, D., Rogers, J., Webster, M., Farinholt, K., Friedersdorf, F., Pepi, M., and Ghoshal, A., 2018, "Novel Approach of Wavelet Analysis for Nonlinear Ultrasonic Measurements and Fatigue Assessment of Jet Engine Components," AIP Conference Proceedings, Provo, UT, July 16–21, pp. 1–11.
[30] Scott, K., Kim, J.-Y., and Jacobs, L. J., 2018, "Signal Processing Methods for Second Harmonic Generation in Thin Specimens," NDT&E Int., **95**, pp. 57–64.
[31] Cantrell, J., 1980, "Generalized Gruneisen Tensor From Solid Nonlinearity Parameters," Phys. Rev. B, **21**(10), pp. 4191–4195.
[32] Joharapurkar, D., and Breazeale, M., 1990, "Nonlinear Parameter, Nonlinearity Constant, and Frequency Dependence of Ultrasonic Attenuation in GaAs," J. Appl. Phys., **67**(1), pp. 76–80.
[33] Joharapurkar, D., Gerlich, D., and Breazeale, M., 1992, "Temperature Dependence of Elastic Nonlinearities in Single-Crystal Gallium Arsenide," J. Appl. Phys., **72**(6), pp. 2002–2008.
[34] Rollins, F. R., 1965, "Phonon Interactions at Ultrasonic Frequencies," Proc. IEEE, **53**(10), pp. 1534–1539.
[35] Cantrell, J., 2006, "Quantitative Assessment of Fatigue Damage Accumulation in Wavy Slip Metals From Acoustic Harmonic Generation," Philos. Mag., **86**(11), pp. 1539–1554.
[36] Cantrell, J., 2009, "Nondestructive Evaluation of Metal Fatigue Using Nonlinear Ultrasonics," Review of Progress in QNDE, Chicago, IL, July 20–25, pp. 19–32.
[37] Wu, B., Yan, B.-S., and He, C.-F., 2011, "Nonlinear Ultrasonic Characterizing Online Fatigue Damage and In Situ Microscopic Observation," Trans. Nonferrous Met. Soc. China, **21**(12), pp. 2597–2604.
[38] Matikas, T., 2010, "Damage Characterization and Real-Time Health Monitoring of Aerospace Materials Using Innovative NDE Tools," J. Mater. Eng. Perform., **19**(5), pp. 751–760.
[39] Hikata, A., Chick, B., and Elbaum, C., 1963, "Effect of Dislocations on Finite Amplitude Ultrasonic Waves in Aluminum," Appl. Phys. Let., **3**(11), pp. 195–197.
[40] Van Buren, A., and Breazeale, M., 1968, "Reflection of Finite-Amplitude Ultrasonic Waves. I. Phase Shift," J. Acoust. Soc. Am., **44**(4), pp. 1014–1020.
[41] Adamczyk, K., Stokkan, G., and Di Sabatino, M., 2018, "Guidelines for Establishing an Etching Procedure for Dislocation Density Measurements on Mulicrystalline Silicone Samples," MethodsX, **5**, pp. 1178–1186.